



PUBLISHED FOR SISSA BY SPRINGER

RECEIVED: June 11, 2015

REVISED: October 26, 2015

ACCEPTED: December 17, 2015

PUBLISHED: January 8, 2016

Interference effects in Higgs production through Vector Boson Fusion in the Standard Model and its singlet extension

Alessandro Ballestrero^a and Ezio Maina^{a,b}

^a*INFN, Sezione di Torino,
Via Giuria 1, 10125 Torino, Italy*

^b*Dipartimento di Fisica, Università di Torino,
Via Giuria 1, 10125 Torino, Italy*

E-mail: ballestrero@to.infn.it, maina@to.infn.it

ABSTRACT: Interference effects play an important role in Electroweak Physics. They are responsible for the restoration of unitarity at large energies. When, as is often the case, higher order corrections are only available for some particular subamplitude, interferences need to be carefully computed in order to obtain the best theoretical prediction. It has been recently pointed out in gluon fusion that whenever more than one neutral, \mathcal{CP} even, scalars are present in the spectrum large cancellations can occur. We extend these studies to Vector Boson Scattering, examining interference effects in the Higgs sector in the Standard Model and its one Higgs Singlet extension. Already in the SM there is a significant difference between the results obtained considering only s -channel Higgs exchange and those obtained from the full set of scalar exchange diagrams. In the 1HSM these effects are modulated by the interference between the two neutral Higgses. The full interference between the heavy Higgs diagrams and the rest of the amplitude, which is the sum of light Higgs exchange diagrams and of those diagrams in which no Higgs appear, is very small for values of the mixing angle compatible with the experimental constraints.

KEYWORDS: Higgs Physics, Beyond Standard Model, Standard Model

ARXIV EPRINT: [1506.02257](https://arxiv.org/abs/1506.02257)

Contents

1	Introduction	1
2	The singlet extension of the Standard Model	3
3	New features in PHANTOM	4
4	Notation and details of the calculation	5
5	Higgs mediated Vector Boson Scattering signal in the SM	7
6	Higgs mediated Vector Boson Scattering signal in the 1HSM	9
7	Full processes	11
8	Cancellation of the heavy Higgs interferences	15
9	Conclusions	17

1 Introduction

Now that a resonance has been discovered at about 125 GeV [1, 2], the race is on to measure all its properties. All studies based on LHC Run I data are consistent with the hypothesis that the new particle is indeed the Standard Model Higgs boson. The mass is already known with an uncertainty smaller than two per mill from the latest published analyses [3, 4] and the signal strengths $\mu^i = \sigma^i/\sigma_{\text{SM}}^i$, where i runs over the decay channels, are known to about 10 to 20% [3, 5, 6]. There is still room for more complicated Higgs sectors but compatibility with experimental results is severely restricting their parameter space [7]. In Run II, larger luminosity and energy will provide more precise measurements of the characteristics of the new particle and extend the mass range in which other scalars can be searched for.

Lately, a lot of attention has been paid to the prospects of detailed studies of off-shell Higgs contributions, which are larger than could naively be expected [8]. On the one hand, at large energies, Higgs exchange unitarizes processes like Vector Boson Scattering (VBS) and fermion pair annihilation to Vector Bosons which would otherwise diverge. On the other hand, the comparison of off-shell and peak cross sections can provide limits on the total width of the Higgs [9–15]. Both aspects are sensitive to BSM physics through direct production of new states and through their contributions in loops.

If additional neutral scalars are present in the physical spectrum, non trivial interference effects have been demonstrated in Gluon Gluon Fusion (GGF) processes [16–19].

It is quite natural to extend these studies to VBS which has been traditionally regarded as the ultimate testing ground of the ElectroWeak Symmetry Breaking mechanism. The ratio of the Higgs production cross section in Vector Boson Fusion (VBF) to the cross section in gluon fusion grows for larger Higgs masses and, as a consequence, the importance of VBF as a discovery channel for new scalar resonances of an extended Higgs sector increases. VBF is not affected by BSM physics through loops [20], therefore it can be argued that the limits it provides on the Higgs width are less model dependent than those obtained in GGF. It is well known that interference effects between Higgs exchange diagrams and all other ones are large in VBF. In the next few years, Vector Boson Fusion will be studied in much greater detail than it was possible with the limited statistics collected in Run I.

There is one aspect in which the Higgs exchange contribution to VBF differs from the GGF case: the set of diagrams which dominate the on-shell case, that is the usual production times decay mechanism, $pp \rightarrow jjH \rightarrow jjVV$, is different from the set of diagrams which is needed to describe the off-shell contribution. In general, in the latter case, there are additional diagrams in which the Higgs field is exchanged in the u -, t -channel which cannot be ignored and significantly modify the predictions based on a naive continuation of s -channel exchange.

Since the landscape of possible extensions of the SM Higgs sector is quite complicated, it makes sense to examine the simplest renormalizable enlargement, that is the one Higgs Singlet Model (1HSM). It introduces one additional real scalar field which is a singlet under all SM gauge groups. The 1HSM has been extensively investigated in the literature [16–19, 21–46]. Recently, a great deal of activity has concentrated on establishing the restrictions imposed on its parameter space by theoretical and experimental constraints [39, 40, 43, 46]; on interference effects between the two neutral Higgs fields and with the continuum [17–19] and on possible consequences on the determination of the Higgs width through a measurement of the off-shell Higgs cross section [16, 44], as proposed in ref. [9].

In Run I VBF was a small fraction of the total diboson cross section. To the best of our knowledge, all experimental analyses so far have treated VBF as a superposition of a Higgs signal times decay sample to the continuum. Part of the appeal of this approach is that higher order corrections can be applied to the signal. ElectroWeak corrections to $pp \rightarrow jjH$ are available at NLO [47, 48]. QCD NLO contributions have been presented in [49–51]. QCD corrections to the total cross section are known almost exactly at NNLO [52, 53] using the structure function approach. NNLO correction to differential distribution have been recently obtained [54]. It should always be kept in mind, however, that the interference between Higgs fields of different masses will also be present in VBS and modulate the cancellations which restore unitarity, producing non negligible modifications to the cross section and to the resonance shape of the heavier scalars.

Since no public MC is available for VBS in the 1HSM, we have upgraded PHANTOM [55], allowing for the simulation of the 1HSM and more generally for the presence of two neutral \mathcal{CP} even scalars.

In this paper we apply this new tool to study interference effects in $pp \rightarrow jjl^+l^-l'^+l'^-$ and $pp \rightarrow jjl^-\bar{\nu}_l l'^+\nu_{l'}$ production, where both l and l' can be either an electron or a muon, $l \neq l'$. This is a case study rather than a complete analysis and we are aware that rates

are expected to be small [15, 56]. A careful investigation of all channels, including the semileptonic ones and exploiting all techniques to identify vector bosons decaying hadronically, will be required to assess the observability of the 1HSM through VBF in Run II and beyond.

2 The singlet extension of the Standard Model

In the following we consider the singlet extension of the SM in the notation of ref. [39]. A real $SU(2)_L \otimes U(1)_Y$ singlet, S , is introduced and the term:

$$\mathcal{L}_s = \partial^\mu S \partial_\mu S - \mu_1^2 \Phi^\dagger \Phi - \mu_2^2 S^2 + \lambda_1 (\Phi^\dagger \Phi)^2 + \lambda_2 S^4 + \lambda_3 \Phi^\dagger \Phi S^2. \quad (2.1)$$

is added to the SM Lagrangian, where Φ is the usual Higgs doublet. \mathcal{L}_s is gauge invariant and renormalizable. A \mathcal{Z}_2 symmetry, $S \leftrightarrow -S$, which forbids additional terms in the potential is assumed. A detailed discussion of the 1HSM without \mathcal{Z}_2 symmetry can be found in refs. [23, 25, 38, 41, 42].

The neutral components of these fields can be expanded around their respective Vacuum Expectation Values:

$$\Phi = \begin{pmatrix} G^\pm \\ \frac{v_d + l^0 + iG^0}{\sqrt{2}} \end{pmatrix} \quad S = \frac{v_s + s^0}{\sqrt{2}}. \quad (2.2)$$

The minimum of the potential is achieved for

$$\mu_1^2 = \lambda_1 v_d^2 + \frac{\lambda_3 v_s^2}{2}; \quad \mu_2^2 = \lambda_2 v_s^2 + \frac{\lambda_3 v_d^2}{2}, \quad (2.3)$$

provided

$$\lambda_1, \lambda_2 > 0; \quad 4\lambda_1 \lambda_2 - \lambda_3^2 > 0. \quad (2.4)$$

The mass matrix can be diagonalized introducing new fields h and H :

$$h = l^0 \cos \alpha - s^0 \sin \alpha \quad \text{and} \quad H = l^0 \sin \alpha + s^0 \cos \alpha \quad (2.5)$$

with $-\frac{\pi}{2} < \alpha < \frac{\pi}{2}$.

The masses are

$$M_{h,H}^2 = \lambda_1 v_d^2 + \lambda_2 v_s^2 \mp |\lambda_1 v_d^2 - \lambda_2 v_s^2| \sqrt{1 + \tan^2(2\alpha)}, \quad \tan(2\alpha) = \frac{\lambda_3 v_d v_s}{\lambda_1 v_d^2 - \lambda_2 v_s^2}, \quad (2.6)$$

with the convention $M_H^2 > M_h^2$.

The Higgs sector in this model is determined by five independent parameters, which can be chosen as

$$m_h, m_H, \sin \alpha, v_d, \tan \beta \equiv v_d/v_s, \quad (2.7)$$

where the doublet VEV is fixed in terms of the Fermi constant through $v_d^2 = G_F^{-1}/\sqrt{2}$. Furthermore one of the Higgs masses is determined by the LHC measurement of 125.02 GeV. Therefore, three parameters of the model, M_H , $\sin \alpha$, $\tan \beta$, are at present undetermined.

The Feynman rules for the 1HSM have been derived using FeynRules [57, 58].¹

It should be mentioned that allowing a discrete symmetry to be spontaneously broken, as is the case in the simplified model considered here when the singlet field S has a non zero vacuum expectation value, will introduce potentially problematic cosmic domain walls [60–65]. These considerations, however have little bearing on the paper’s main point.

For future reference, we report the expression of the tree level partial width for the decay of the heavy scalar into two light ones:

$$\Gamma(H \rightarrow hh) = \frac{e^2 M_H^3}{128\pi M_W^2 s_W^2} \left(1 - \frac{4M_h^2}{M_H^2}\right)^{\frac{1}{2}} \left(1 + \frac{2M_h^2}{M_H^2}\right)^2 s_\alpha^2 c_\alpha^2 (c_\alpha + s_\alpha \tan \beta)^2 \quad (2.8)$$

and those of the width of both scalars:

$$\Gamma_h = \Gamma^{\text{SM}}(M_h)c_\alpha^2, \quad \Gamma_H = \Gamma^{\text{SM}}(M_H)s_\alpha^2 + \Gamma(H \rightarrow hh) \quad (2.9)$$

where $c_\alpha = \cos \alpha$, $s_\alpha = \sin \alpha$.

The strongest limits on the parameters of the 1HSM [40, 43, 46] come from measurements of the coupling strengths of the light Higgs [3, 5–7], which dominate for small masses of the heavy Higgs, and from the contribution of higher order corrections to precision measurements, in particular to the mass of the W boson [40], which provides the tightest constraint for large M_H . The most precise result for the overall coupling strength of the Higgs boson from CMS [3] reads

$$\hat{\mu} = \hat{\sigma}/\sigma_{\text{SM}} = 1.00 \pm 0.13. \quad (2.10)$$

Therefore the absolute value of $\sin \alpha$ cannot be larger than about 0.4. This is in agreement with the limits obtained in ref. [40, 43, 46] which conclude that the largest possible value for the absolute value of $\sin \alpha$ is 0.46 for M_H between 160 and 180 GeV. This limit becomes slowly more stringent for increasing heavy Higgs masses reaching about 0.2 at $M_H = 700$ GeV.

3 New features in PHANTOM

PHANTOM has been upgraded to allow for the presence of two neutral \mathcal{CP} even scalars. The parameters which control how the Higgs sector is simulated, with masses and widths expressed in GeV, are:

- **rmh**: light Higgs mass. If **rmh** < 0 all light and heavy Higgs exchange diagrams are set to zero.

¹The corresponding UFO file [59], which allows the simulation at tree level of any process in the model, can be downloaded from <http://personalpages.to.infn.it/~maina/Singlet>.

- **gamh**: light Higgs width. If $\text{gamh} < 0$ the width is computed internally following the prescription of ref. [66] and multiplied by $\cos^2 \alpha$ if working in the 1HSM.

Within the SM framework, it is also possible to modify all Higgs couplings by a common factor setting the parameter **ghfactor**.

The parameter **i_singlet** selects whether PHANTOM performs the calculations in the SM (**i_singlet**=0) or in the 1HSM (**i_singlet**=1). If the 1HSM is selected the following inputs are required:

- **rmhh**: heavy Higgs mass. If $\text{rmhh} < 0$ all heavy Higgs exchange diagrams are set to zero.
- **rcosa**: the cosine of the mixing angle α .
- **tgbeta**: $\tan \beta$.
- **gamhh**: heavy Higgs width. If $\text{gamhh} < 0$ the width is computed internally following the prescription of ref. [66] and then multiplied by $\sin^2 \alpha$. $\Gamma(H \rightarrow hh)$, eq. (2.8), is then added to the result.

Moreover the contribution of the Higgs exchange diagrams can be computed separately, both in the SM and in the 1HSM, setting the following flag:

- **i_signal**: if **i_signal** = 0 the full matrix element is computed.
If **i_signal** > 0 only a set of Higgs exchange diagrams are evaluated at $\mathcal{O}(\alpha_{EM}^6)$:
 - **i_signal** = 1: s -channel exchange contributions.
 - **i_signal** = 2: all Higgs exchange contributions to VV scattering.
 - **i_signal** = 3: all Higgs exchange contributions to VV scattering plus the Higgsstrahlung diagrams with $h, H \rightarrow VV$.

4 Notation and details of the calculation

We are going to present results, at the 13 TeV LHC, for $pp \rightarrow jj e^+ e^- \mu^+ \mu^-$ and $pp \rightarrow jj e^- \bar{\nu}_e \mu^+ \nu_\mu + c.c$ production. We have identified the light Higgs h with the resonance discovered in Run I and set its mass to 125 GeV, concentrating on the scenario in which the heavy Higgs H is still undetected.

Samples of events have been generated with PHANTOM using CTEQ6L1 parton distribution functions [67]. The ratio of vacuum expectation values, $\tan \beta$, has been taken equal to 0.3 for $M_H = 600$ GeV and $M_H = 900$ GeV, and equal to 1.0 for $M_H = 400$ GeV. This corresponds, using eq. (2.8) for the $H \rightarrow hh$ width and ref. [66] for the SM Higgs width, to $\Gamma_H = 4.08$ GeV for $M_H = 400$ GeV, $s_\alpha = 0.3$; $\Gamma_H = 6.45$ GeV for $M_H = 600$ GeV and $s_\alpha = 0.2$; $\Gamma_H = 89.14$ GeV for $M_H = 900$ GeV and $s_\alpha = 0.4$.

The charged leptons are required to satisfy:

$$p_{Tl} > 20 \text{ GeV}, \quad |\eta_l| < 2.5, \quad m_{l+l-} > 20 \text{ GeV} \quad (4.1)$$

while the cuts on the jets are:

$$p_{Tj} > 20 \text{ GeV}, \quad |\eta_j| < 5.0, \quad m_{j_1 j_2} > 400 \text{ GeV}, \quad \Delta\eta_{j_1 j_2} > 2.0. \quad (4.2)$$

For processes with two charged leptons and two neutrinos in the final state we further impose:

$$\not{p}_T > 20 \text{ GeV}, \quad |m_{bl+\nu_l} - m_{\text{top}}| > 10 \text{ GeV}, \quad |m_{\bar{b}l-\bar{\nu}_l} - m_{\text{top}}| > 10 \text{ GeV}. \quad (4.3)$$

The latter requirement eliminates the large contribution from EW and QCD top production.

In the following we will discuss various sets of diagrams and different groups of processes, therefore, we introduce our naming convention. We split the amplitude A , for each process, as:

$$A = A_B + A_h + A_H \equiv A_{\text{1HSM}}, \quad (4.4)$$

where $A_{h/H}$ denote the set of diagrams in which a light/heavy Higgs is exchanged, e.g. diagrams (a) and (b) in figure 1, and A_B the set of diagrams in which no Higgs is present, e.g. diagrams (c) and (d), which we will also refer to as background or noHiggs amplitude. $A_{h/H}$ contain all VBS diagrams in which a h/H Higgs interacts with the vector bosons. They also contain a small set of additional diagrams, e.g. Higgsstrahlung ones. These can be ignored for all practical purposes since their contribution, with the present cut on the minimum invariant mass of the two jets which forbids them to resonate at the mass of a weak boson, is very small. From time to time we will refer to the sum of subamplitudes using the notation $A_{ij} = A_i + A_j$. A similar convention will be adopted for differential or total cross sections so that σ_i corresponds to the appropriate integral over phase space of $|A_i|^2$ summed over all contributing processes. As an example, σ_{Bh} is obtained integrating the modulus squared of $A_{Bh} = A_B + A_h$, the coherent sum of the diagrams without any Higgs and those involving the light Higgs only. $\sigma_{\text{1HSM}} \equiv \sigma$ will denote the full (differential) cross section.

The VBS diagrams in $A_{h/H}$ can be further classified by the pair of vector bosons which initiate the scattering and by the final state pair. In this paper we concentrate on $pp \rightarrow jjl^+l^-l'^+l'^-$ and $pp \rightarrow jjl^-\bar{\nu}_l l'^+\nu_{l'}$ production so that the only instances of VBS which appear correspond to $ZZ \rightarrow ZZ$ ($Z2Z$) and $WW \rightarrow ZZ$ ($W2Z$) for the $jjl^+l^-l'^+l'^-$ case and to $ZZ \rightarrow WW$ ($Z2W$) and $WW \rightarrow WW$ ($W2W$) for the $jjl^-\bar{\nu}_l l'^+\nu_{l'}$ final state.

The $W2Z$ and $Z2W$ sets are particularly simple because the Higgs fields appear only in the s -channel. In the $Z2Z$ case scalars are exchanged in the s -, t - and u -channel, while in the $W2W$ set the Higgses contribute in the s - and t -channel.

Some of the processes contributing to $4ljj$ production include only the $Z2Z$ subprocess, for instance $uc \rightarrow uce^+e^-\mu^+\mu^-$; others only contain the $W2Z$ subprocess, for instance $us \rightarrow dce^+e^-\mu^+\mu^-$. Finally there is a class of processes, like $ud \rightarrow ude^+e^-\mu^+\mu^-$, which include both kind of subdiagrams. They will be called $P(Z2Z)$, $P(W2Z)$ and $P(Z2Z + W2Z)$ processes respectively.

Some processes leading to the $2l2\nu jj$ final state contain only the $Z2W$ set, for instance $u\bar{c} \rightarrow u\bar{c}e^+\bar{\nu}_e\mu^-\nu_\mu$; others only contain the $W2W$ set, like $u\bar{c} \rightarrow d\bar{s}e^+\bar{\nu}_e\mu^-\nu_\mu$. A third

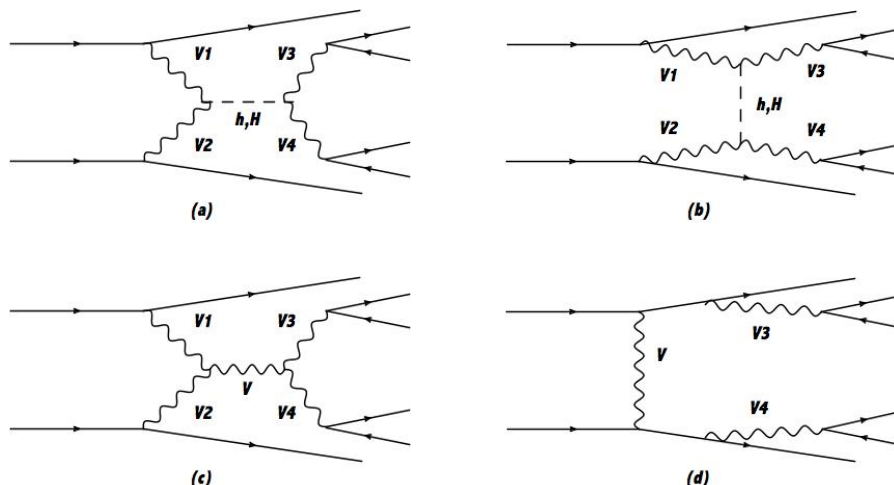


Figure 1. Some Feynman diagrams contributing to $pp \rightarrow jjl^+l^-l'^+l'^-$ and $pp \rightarrow jjl^-\bar{\nu}_l l'^+\nu_l$. Diagram (a) and (b) describe s- and t/u-channel Higgs exchange in VBS. Diagram (c) contributes to VBS but does not involve the Higgs. Diagram (d) does not contain VBS subdiagrams.

group of reactions includes both kind of subdiagrams, for instance $ud \rightarrow ude^+\bar{\nu}_e\mu^-\nu_\mu$. They will be called $P(Z2W)$, $P(W2W)$ and $P(Z2W + W2W)$ processes, respectively.

The $4lj$ final state has a tiny branching ratio but is very clean. The invariant mass of the leptonic system can be measured with high precision and small background.

In the $2l2\nu jj$ final state, the two charged leptons will be required to belong to different families and charges so that the final state can be thought of as containing a W^+W^- pair. The $2l2\nu jj$ final state has a much larger cross section. However, the invariant mass of the WW system cannot be reconstructed and it can only be experimentally analyzed in terms of the transverse mass of the leptonic system.

In the following we will examine these reactions with the aim of clarifying the role and size of interference effects in VBS, disregarding their actual observability at the LHC which would require a detailed study of all available channels and a careful assessment of reducible and irreducible backgrounds. Some of the distributions we present are not accessible in practice but are nonetheless useful tools for a first theoretical estimate of interference effects in different contexts.

5 Higgs mediated Vector Boson Scattering signal in the SM

We begin our presentation with a discussion of the small set of SM diagrams in which VBS is mediated by Higgs exchange.

On the left hand side of figure 2, we show in red the mass distribution for the $4lj$ final state obtained taking into account only the diagrams with s-channel Higgs exchange and in blue the result when the full set of Higgs exchange diagrams is included. The contribution of the $P(Z2Z)$ processes is shown separately: in purple the result due solely to s-channel Higgs exchange and in violet the result obtained from the sum of all three channels. Here

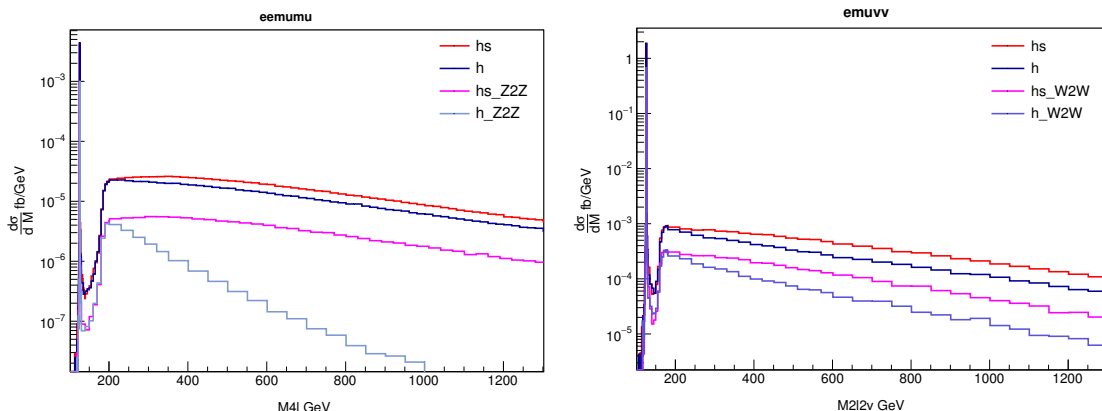


Figure 2. Invariant mass distribution of the four lepton system for the 4lj final state (left) and the 2l2νjj final state (right) in the SM. In red and purple the mass distribution obtained taking into account only the diagrams with s -channel Higgs exchange and in blue and violet the result when the full set of Higgs exchange diagrams is included. On the left(right), the two contributions of the $P(Z2Z)(P(W2W))$ processes is shown separately.

and in the following, for readability, we use bins of different size around the peaks and in the off-peak regions.

On the right hand side of figure 2 we show the corresponding results for the 2l2νjj final state. In this case, it is the contribution of the $P(W2W)$ processes which is shown separately.

We see that there is a significant difference between the curves obtained considering only s -channel Higgs exchange and those obtained from the full set of scalar exchange diagrams. This implies a conspicuous negative interference between the Higgs exchange diagrams in $P(Z2Z)$ and $P(W2W)$ processes. This interference is so large that it significantly modifies the result obtained when all processes are summed, even though there are reactions which contribute substantially to the total which are not affected at all by these effects like $P(W2Z)$ and $P(Z2W)$ processes and others, the $P(Z2W + W2W)$ and $P(Z2Z + W2Z)$ groups, which are affected only partially.

Large cancellations in $P(Z2Z)$ processes are expected. On shell $ZZ \rightarrow ZZ$ scattering is zero in the absence of the Higgs and therefore does not violate unitarity at high energy. As a consequence the corresponding Higgs diagrams, each of which grows as the invariant mass squared of the process, must combine in such a way that their sum is actually asymptotically finite. At large energy, the longitudinal polarization vector of a Z boson of momentum p^μ can be identified with p^μ/M_Z and the sum of the three Feynman diagrams describing the scattering behaves as $s^2/s+t^2/t+u^2/u = s+t+u \approx 0$. It is however surprising that the cancellation grows so rapidly, above threshold, with the mass of the ZZ pair and becomes substantial already at moderate invariant masses. For $M_{ZZ} = 500$ GeV the square of the three Higgs exchange diagrams is an order of magnitude smaller than the result obtained from s -channel exchange alone. The same cancellation takes place in the amplitude of the $P(Z2Z + W2Z)$ processes, while the $P(W2Z)$ sector is unaffected. In the sum of all processes the interference decreases the SM result for s -channel Higgs exchange by about 25%.

Interference effects are present also in $P(W2W)$ processes, as shown in the right hand side of figure 2. They are less prominent than in the $P(Z2Z)$ case. The same cancellation takes place in the amplitude of the $P(Z2W + W2W)$ processes, while the $P(Z2W)$ sector is unaffected. Summing all processes, the difference between the result obtained from the single s -channel exchange diagram (red) and the full set (blue) is larger than for $4ljj$ production because WW initiated scatterings are more frequent than ZZ ones for the $2l2\nu jj$ final state. The interference decreases the SM result for s -channel Higgs exchange by about 30%. The on shell reaction $W^+W^- \rightarrow W^+W^-$ violates unitarity in a Higgsless theory when the W 's are longitudinally polarized. Therefore Higgs exchange diagrams are necessary to restore unitarity and the cancellation can only be partial. There is no u -channel exchange, so, at large energy, the sum of the two diagrams behaves as $t^2/t + s^2/s = t + s \approx -u$.

These results imply that, when producing Monte Carlo templates for the analysis of off shell Higgs production, it is mandatory to include the full set of Higgs exchange diagrams. This is coherent with the Caola-Melnikov method which isolates all terms in the amplitude which are proportional to the same power of the Higgs couplings. As a consequence all Higgs exchange diagrams need to be taken as a unit, regardless of the channel in which the exchange takes place.

QCD radiative corrections in VBF are small. They are crucial in reducing the scale dependence of the predictions to the 5-10% level. NNLO corrections bring the uncertainty down to about 2%. When aiming for high accuracy, interference effects, which have a comparable if not larger impact, cannot be ignored.

6 Higgs mediated Vector Boson Scattering signal in the 1HSM

We now turn to the 1HSM. In this case there are two sets of Higgs exchange diagrams, one for each of the two Higgs fields in the model. In general, an amplitude involving a single Higgs exchange can be written schematically as

$$A = A_s P(s) + A_t P(t) + A_u P(u) + A_0 \tag{6.1}$$

where A_0 does not involve the scalar fields and

$$P(x) = \left(\frac{c_\alpha^2}{x - M_h^2 + i\Gamma_h M_h} + \frac{s_\alpha^2}{x - M_H^2 + i\Gamma_H M_H} \right) \tag{6.2}$$

The real parts of the two terms in $P(s)$ interfere destructively for $M_h^2 < q^2 < M_H^2$ and constructively for $q^2 < M_h^2$ and $M_H^2 < q^2$. In the region around $s = M_h^2$ the heavy Higgs amplitude becomes as large or larger than the light Higgs one and the interference can be substantial. In $P(t)$ and $P(u)$ the two terms always have the same sign. Moreover, the heavy Higgs amplitude will be decreased in comparison with the light Higgs one by the larger value of the mass. As a consequence, while technically interference effects are present in these subamplitudes, they are expected to be much less significant. Only at large energies the masses can be neglected and the sum of the two contributions reproduce the SM result in each channel, as required by unitarity.

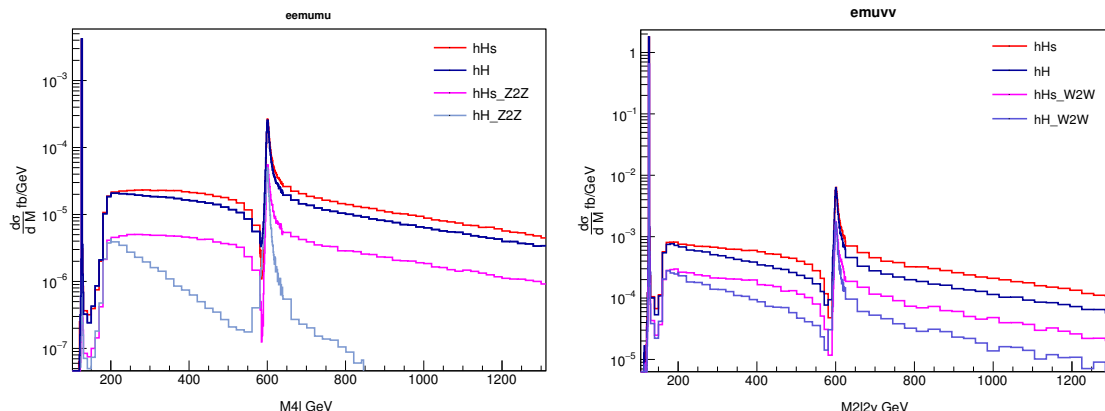


Figure 3. Invariant mass distribution of the four lepton system for the 4ljj final state (left) and the 2l2νjj final state (right) in the 1HSM with $M_H = 600$ GeV and $s_\alpha = 0.2$, $\tan\beta = 0.3$. In red and purple the mass distribution obtained taking into account only the diagrams with s -channel Higgs exchange and in blue and violet the result when the full set of Higgs exchange diagrams is included. On the left(right), the two contributions of the $P(Z2Z)(P(W2W))$ processes is shown separately.

We present results for selected values of M_H , s_α and $\tan\beta$ but our conclusions are fairly independent of the choice of parameters. In figure 3 we show a number of four lepton mass distributions, for the 4ljj final state on the left and the 2l2νjj final state on the right, for $M_H = 600$ GeV, $s_\alpha = 0.2$ and $\tan\beta = 0.3$. The colors of the histograms in figure 3 follow the convention of figure 2. The red and purple lines refer to pure s -channel exchange. The red one relates to the sum of all processes while the purple one to $P(Z2Z)$ processes (left) and $P(W2W)$ ones (right), only. The blue and violet lines correspond to the sum of all Higgs exchange diagrams. The pattern and size of interference effects among different sets of Higgs exchange diagrams are similar to those in the SM. In addition, all curves in figure 3, in the region around 600 GeV, show an interference pattern between the light and heavy Higgs similar to one present in the GGF case [16–19]. The inclusion of the full set of Higgs exchange diagrams decreases the size of the pure s -channel exchange amplitude over the whole energy range, as in the SM case, with the exception of a small region below the heavy Higgs mass where the interference between the two scalars dominate. It also significantly affects the interference pattern in the neighborhood of M_H . For completeness we notice that in the energy range under consideration, as expected, the diagrams with a heavy Higgs exchange in the t -, u -channels are extremely small compared to the diagram with s -channel exchange.

In figure 4 we compare the invariant mass distribution of the four lepton system for the 4ljj (left) and 2l2νjj (right) final state obtained taking into account the full set of Higgs exchange diagrams in the 1HSM (blue) with the incoherent sum (red) of the Higgs exchange diagrams for Higgs masses of 125 and 600 GeV. The individual contributions of the two Higgs are shown in green and black respectively. The difference between the blue curve and the black and red ones illustrates the deformation of the Breit Wigner distribution induced by interference effects. They are negative in the region below M_H and positive

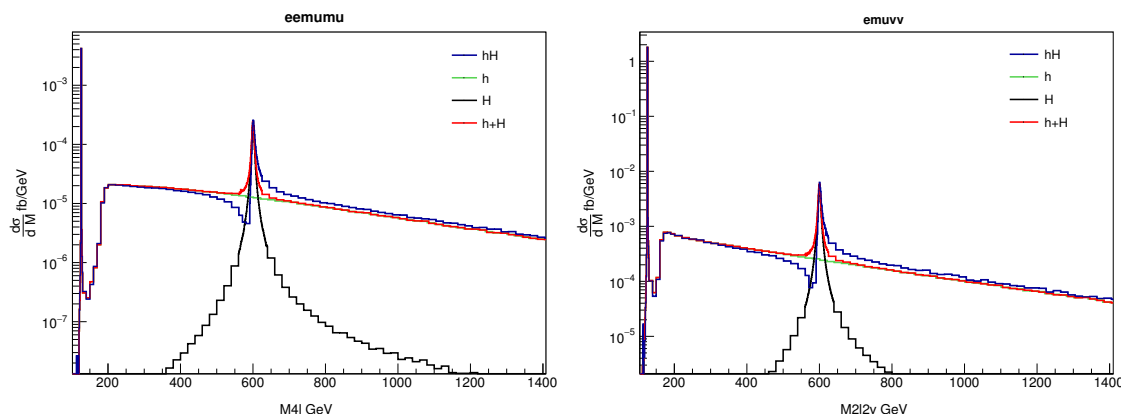


Figure 4. Invariant mass distribution of the four lepton system for the 4ljj final state in the 1HSM with $M_H = 600$ GeV and $s_\alpha = 0.2$, $\tan\beta = 0.3$. In green and black the mass distribution obtained taking into account the full set of Higgs exchange diagrams for Higgs masses of 125 and 600 GeV respectively. In red the incoherent sum of the two contributions. In blue the result of all Higgs diagrams in the 1HSM.

above the heavy Higgs resonance as demonstrated by the comparison of the blue and red histograms. Effects are even larger if only the s -channel exchange is taken into account but from now on we only consider the full set of Higgs exchange diagrams which, even though not gauge invariant and therefore not physically observable, provides a better description of the Higgs contribution in the off shell region.

Clearly, this interference between different Higgs fields is not a peculiarity of the Singlet Model. It will indeed occur in any theory with multiple scalars which couple to the same set of elementary particles, albeit possibly with different strengths.

7 Full processes

After our presentation of the interplay of the different sets of Higgs exchange diagrams, we move to the discussion of the actual cross section for the production of a Singlet Model heavy Higgs at the LHC. The plot on the left hand side of figure 5 shows the prediction for 4ljj production in the 1HSM (blue) with $M_H = 600$ GeV and $s_\alpha = 0.2$. Charged leptons satisfy the requirements in eq. (4.1) while jets pass the cuts in eq. (4.2). The 1HSM exact result, in blue, is compared with different approximations. The green histograms is the light Higgs plus no-Higgs contribution, $d\sigma_{Bh}/dM$; the red one refers to $d\sigma_{BH}/dM$; the gray one to $d\sigma_B/dM + d\sigma_H/dM$ and the brown one to $d\sigma_B/dM + d\sigma_h/dM + d\sigma_H/dM$. On the right hand side of figure 5 the corresponding curves for the 2l2νjj final state are displayed. None of the approximations in figure 5 approaches the exact result better than about 20% in the region around the heavy scalar peak and they obviously fare even worse at large M_{4l} , with the exception of the green curve which misses only the heavy Higgs subamplitude, which is proportional to s_α^2 and numerically small in this energy range and outside the peak region, though necessary for unitarity. Clearly, neglecting any part of an amplitude requires a great deal of attention and a careful estimate of the resulting discrepancy.

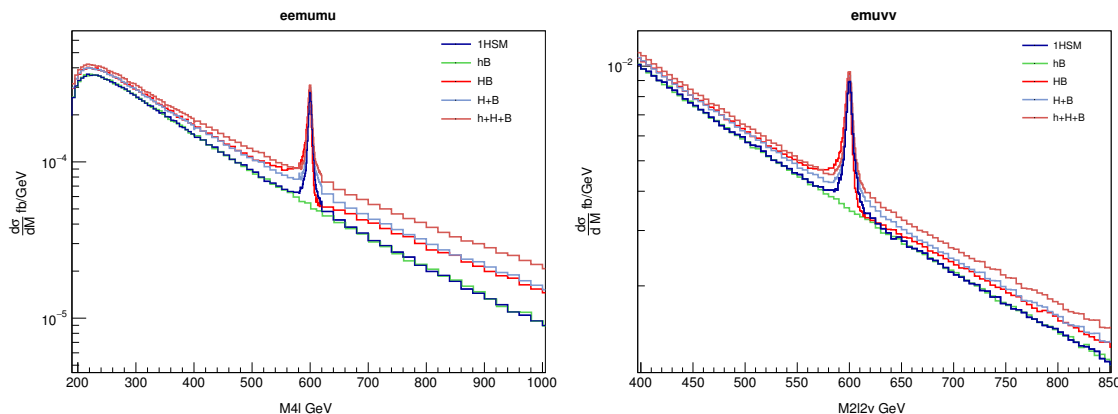


Figure 5. In blue, the invariant mass distribution of the four lepton system for the 4ljj final state (left) and the 2l2νjj final state (right) in the 1HSM with $M_H = 600$ GeV and $s_\alpha = 0.2$. The other curves are different approximations as detailed in the main text.

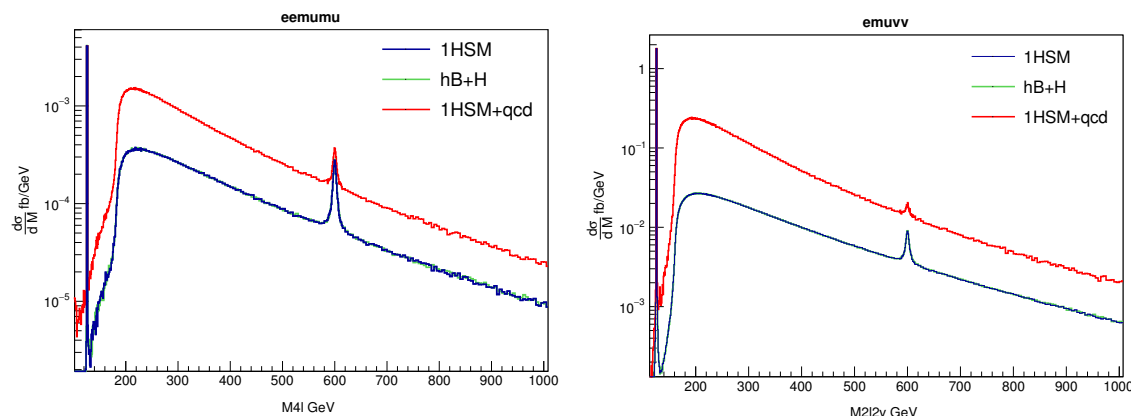


Figure 6. Invariant mass distribution of the four lepton system for the 4ljj final state (left) and the 2l2νjj final state (right) in the 1HSM with $M_H = 600$ GeV and $s_\alpha = 0.2$. The blue histogram is the exact 1HSM result. The green line refers to $d\sigma_{Bh}/dM + d\sigma_H/dM$. The red curve is the sum of the 1HSM result and of the QCD contribution at $\mathcal{O}(\alpha_{EM}^4 \alpha_S^2)$.

There is however a combination of subamplitudes which provides a good approximation to the exact result. In figure 6 the prediction for 4ljj/2l2νjj production in the 1HSM, in blue, is compared with the curve, in green, obtained from the incoherent sum of $d\sigma_{Bh}/dM$ and $d\sigma_H/dM$, both of them computed with 1HSM couplings and widths. The two histograms agree remarkably well over the full mass range. This is particularly meaningful in the region of the heavy Higgs peak where A_H is large: it implies that the interference terms of the heavy Higgs diagrams with A_h and A_B cancel each other to a large degree. For comparison, we also show in red the sum of the full $\mathcal{O}(\alpha_{EM}^6)$ result discussed above and of the QCD contribution at $\mathcal{O}(\alpha_{EM}^4 \alpha_S^2)$. The cross section is a factor of about three larger than the EW result.

As mentioned before, the invariant mass of the W boson pair is not measurable, therefore on the left hand side of figure 7 we show the transverse mass distribution for the 2l2νjj

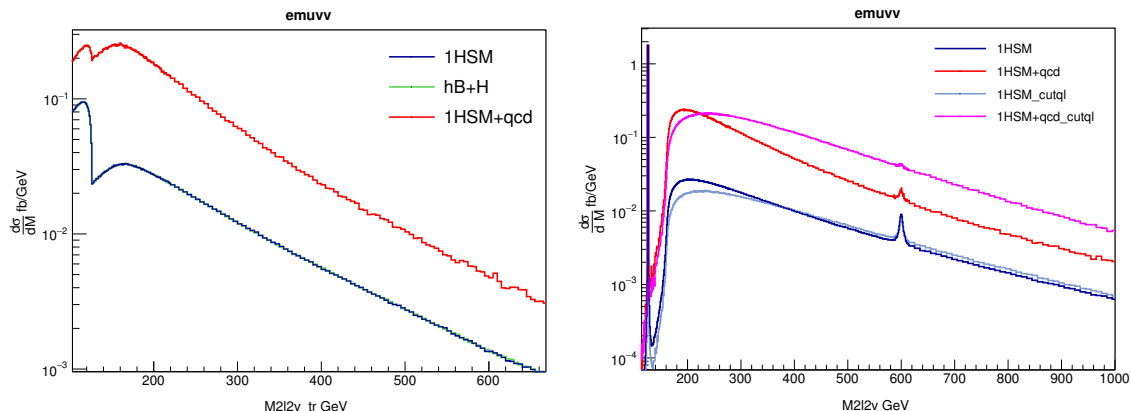


Figure 7. On the left, the transverse mass distribution of the four lepton system for the $2l2\nu jj$ final state in the 1HSM with $M_H = 600$ GeV and $s_\alpha = 0.2$. The blue histogram is the exact 1HSM result. The green line refers to $d\sigma_{Bh}/dM + d\sigma_H/dM$. The red curve is the sum of the 1HSM result and of the QCD contribution at $\mathcal{O}(\alpha_{EM}^4 \alpha_S^2)$. On the right, we compare the distributions obtained with the top veto cut in eq. (4.3) (blue and red lines) with the ones obtained with the requirement $m_{l_1 j_2}, m_{l_2 j_1} > 200$ GeV (gray and purple lines), where l_1, l_2 (j_1, j_2) represent the leptons (jets) of highest and lowest transverse momentum respectively.

final state. The transverse mass is defined as:

$$(M_T^{WW})^2 = (E_{T,u} + E_{T,miss})^2 - |\vec{p}_{T,u} + \vec{E}_{T,miss}|^2, \quad (7.1)$$

where $E_{T,u} = \sqrt{(\vec{p}_{T,u})^2 + M_u^2}$. The heavy Higgs peak has been completely washed out, as expected. Also in this case, the sum $\sigma_{Bh} + \sigma_H$ describes very well the exact distribution. Clearly the fully leptonic decay of the WW pair can only be considered as a case study. In order to employ the W^+W^-jj channel in the search for additional heavy scalars it will be necessary to consider the semileptonic decays.

On the right hand side, we compare the distributions obtained with the top veto cut in eq. (4.3) with the ones obtained with the more realistic requirement proposed in [15, 68] $m_{l_1 j_2}, m_{l_2 j_1} > 200$ GeV, where l_1, l_2 (j_1, j_2) represent the leptons (jets) of highest and lowest transverse momentum respectively. The blue and red lines refer to the first case for the $\mathcal{O}(\alpha_{EM}^6)$ and $\mathcal{O}(\alpha_{EM}^4 \alpha_S^2)$ cross section, while the gray and purple lines refer to the second set of cuts. The two cuts work equally well for the purely electroweak processes. On the contrary, when the $\mathcal{O}(\alpha_{EM}^4 \alpha_S^2)$ reactions are included, the more realistic one is less effective. However, neither is representative of the full range of variables, from b -tagging to shape variables, which can be used to veto tops.

As a check of the dependence of the effects discussed above on the heavy Higgs mass, in figure 8 we show some results for $4lj$ production in the 1HSM with $M_H = 400$ GeV, $s_\alpha = 0.3$ and $\tan \beta = 1.0$. On the left, the full result, in blue, is compared with different combinations of subamplitudes. The green histograms is the light Higgs plus no-Higgs contribution, $d\sigma_{Bh}/dM$; the red one refers to $d\sigma_{Bh}/dM$; the black one to $d\sigma_B/dM + d\sigma_H/dM$ and the brown one to $d\sigma_B/dM + d\sigma_h/dM + d\sigma_H/dM$. Again, none of these approximations

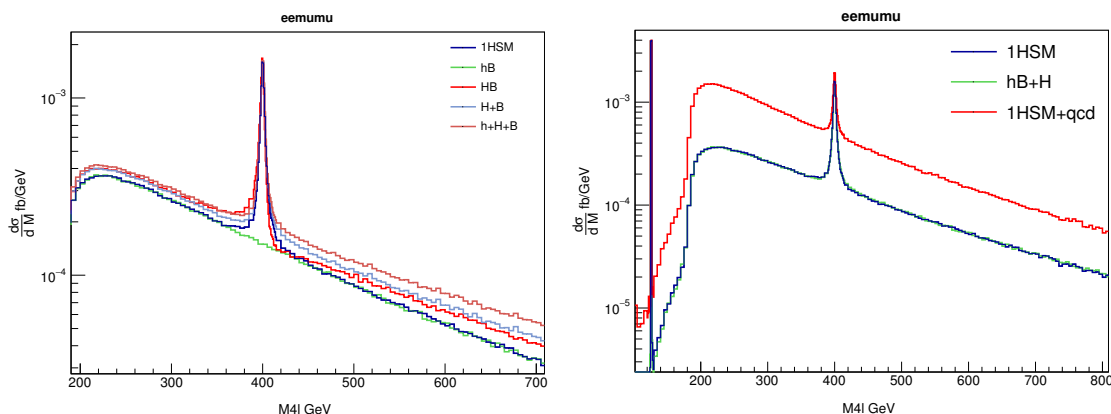


Figure 8. Invariant mass distribution of the four lepton system for the 4ljj final state in the 1HSM with $M_H = 400$ GeV, $s_\alpha = 0.3$ and $\tan\beta = 1.0$. On the left, the 1HSM result, in blue, is compared with different approximations as detailed in the main text. On the right the exact result is compared with $d\sigma_{Bh}/dM + d\sigma_H/dM$, in green. The red curve is the sum of the 1HSM result and of the QCD contribution at $\mathcal{O}(\alpha_{EM}^4 \alpha_S^2)$.

M_H (GeV), s_α	$200 \text{ GeV} < M_{4l} < 1 \text{ TeV}$				$ M_{4l} - M_H < 25 \text{ GeV}$			
	σ	σ_{Bh}	$\sigma_{Bh} + \sigma_H$	σ_{SM}	σ	σ_{Bh}	$\sigma_{Bh} + \sigma_H$	σ_{SM}
400, 0.3, 4l	91.2	81.2	91.3	80.8	17.0	7.5	17.0	7.5
600, 0.2, 4l	83.1	80.8	83.2	80.8	4.8	2.6	4.8	2.7
600, 0.2, 2l2 ν	5565	5510	5567	5509	229	177	230	177

Table 1. Cross sections in attobarns at the LHC with a center of mass energy of 13 TeV. σ refers to the full 1HSM result, while σ_{SM} corresponds to $s_\alpha = 0$. The SM cross section in $|M_{4l} - M_H| < 25$ GeV can be considered as the SM background to the heavy Higgs.

describe satisfactorily the region around the heavy scalar peak. All of them, with the exception of the green curve, lack terms which are crucial for the restoration of unitarity, and progressively diverge from the exact result as the four lepton mass increases. On the right the exact result is compared with $d\sigma_{Bh}/dM + d\sigma_H/dM$. The agreement between the two curves is impressive. In red we show the sum of the full $\mathcal{O}(\alpha_{EM}^6)$ result and of the QCD contribution at $\mathcal{O}(\alpha_{EM}^4 \alpha_S^2)$.

In table 1 we show the cross section in attobarns for two mass intervals: $200 \text{ GeV} < M_{4l} < 1 \text{ TeV}$, which roughly coincides with the range employed so far by the experimental collaborations to set limits on the presence and couplings of additional scalars, and $|M_{4l} - M_H| < 25 \text{ GeV}$, as an indication of the possible effects on an analysis in smaller mass bins which requires high luminosity. σ refers to the full 1HSM result, while σ_{SM} corresponds to $s_\alpha = 0$.

We notice that $\sigma_{Bh} \approx \sigma_{SM}(s_\alpha = 0)$ in both intervals. The only difference between the two results is that in the first case the light Higgs couplings are scaled by c_α . Therefore, the off shell predictions are hardly affected by this modification.

The incoherent sum $\sigma_{Bh} + \sigma_H$ agrees with the exact result in all cases also when integrated over.

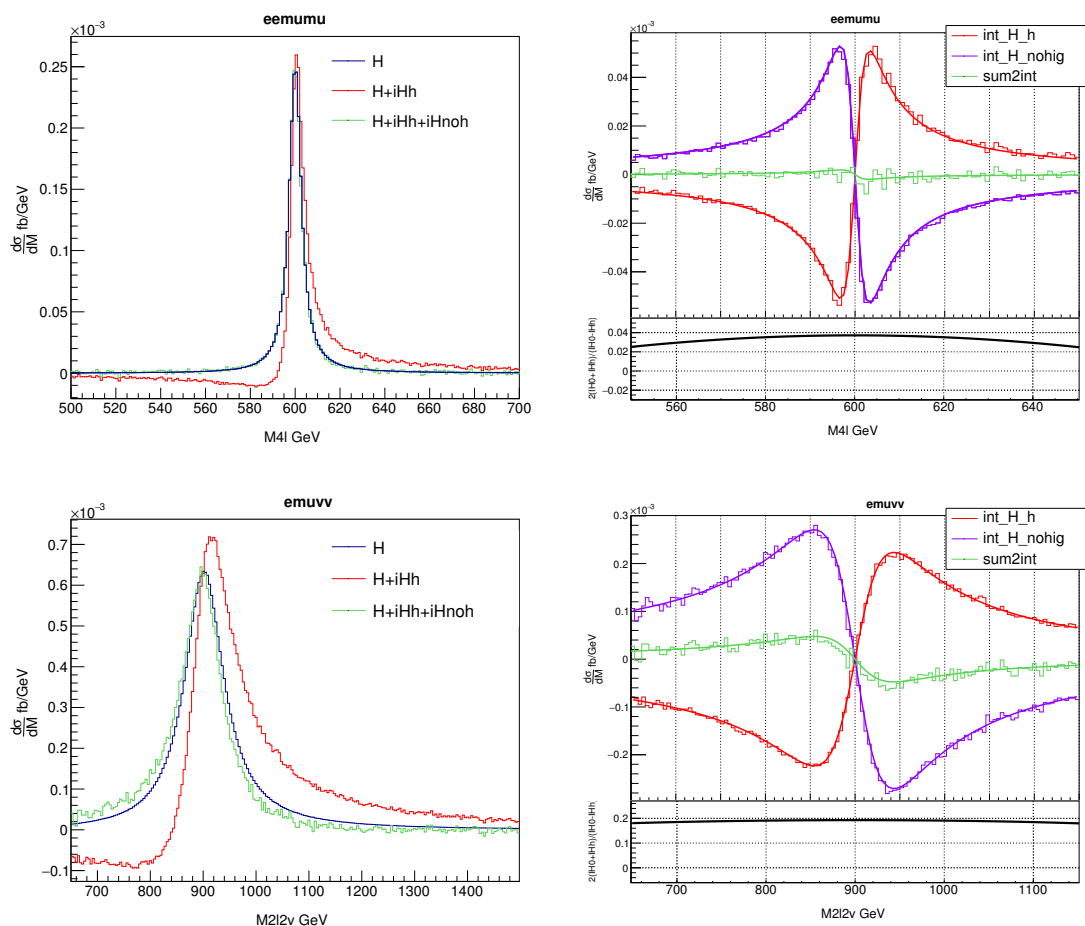


Figure 9. In the upper row, the invariant mass distribution of the four lepton system for the 4l final state in the 1HSM with $M_H = 600$ GeV and $s_\alpha = 0.2$. In the lower row the corresponding plots for the 2l2νjj final state with $M_H = 900$ GeV and $s_\alpha = 0.4$. On the left we show $d\sigma_H/dM$ (blue), $d\sigma_H/dM + dI_{hH}/dM$ (red) and $d\sigma_H/dM + dI_{hH}/dM + dI_{BH}/dM$ (green). On the right we show dI_{hH}/dM (red), dI_{BH}/dM (violet) and $dI_{hH}/dM + dI_{BH}/dM$ (green).

The predicted number of heavy Higgs events at the LHC in the three cases detailed in table 1, taking into account an additional factor of two when summing over all combinations of light leptons, is 6/1/18 for the expected luminosity of 300 fb^{-1} in Run II. The signal to background ratio is of order one. Detecting a 1HSM heavy Higgs in VBF at the LHC will be challenging, even after the high luminosity upgrade.

8 Cancellation of the heavy Higgs interferences

It is noteworthy that the interference terms of the heavy Higgs diagrams with A_h and A_B cancel each other almost exactly for different ranges of invariant mass of the final state vector boson pair and different small amounts of mixing between the light and heavy Higgs. The interference corresponds to the integral of

$$I = 2 \Re(A_H^* \times (A_B + A_h)) = 2 \Re(A_H^* \times (A_B + c_\alpha^2 A_h^{\text{SM}})). \quad (8.1)$$

Since $A_h \propto c_\alpha^2$, the cancellation cannot take place for arbitrary values of the mixing angle α .

In order to investigate further this phenomenon, in figure 9 we isolate the interference terms for different choices of parameters. In the upper row, we show the invariant mass distribution of the four lepton system for the $4l$ final state in the 1HSM with $M_H = 600$ GeV and $s_\alpha = 0.2$. In the lower row the corresponding plots for the $2l2\nu jj$ final state is given with $M_H = 900$ GeV and $s_\alpha = 0.4$, a rather extreme case in view of the allowed parameter space. Defining I_{ij} as the integrated interference between A_i and A_j , on the right we show $d\sigma_{hH}/dM - d\sigma_h/dM - d\sigma_H/dM = dI_{hH}/dM$ (red), $d\sigma_{HB}/dM - d\sigma_B/dM - d\sigma_H/dM = dI_{BH}/dM$ (violet) and $dI_{hH}/dM + dI_{BH}/dM$ (green). On the left we show $d\sigma_H/dM$ in blue, $d\sigma_H/dM + dI_{hH}/dM$ (red) and $d\sigma_H/dM + dI_{hH}/dM + dI_{BH}/dM$ (green).

The plot in the upper left corner shows how, for $M_H = 600$ GeV and $s_\alpha = 0.2$, the interference between the heavy and the light Higgs deforms the Breit-Wigner distribution of the heavy scalar and how the inclusion of the interference between the heavy Higgs and the subamplitude without any Higgs practically eliminates the deformation. The plot on the top right displays the two interferences and their sum, which is much smaller. The red and violet continuous lines are fits to the corresponding histograms with functions of the form:

$$f = A \frac{M_{VV}^2 - M_H^2}{(M_{VV}^2 - M_H^2)^2 + \Gamma_H^2 M_H^2} + B (M_{VV}^2 - M_H^2)^C \quad (8.2)$$

where A , B and C are free parameters. The green continuous line is the sum of the red and violet ones. The lower subplot shows the ratio

$$R = 2 \frac{dI_{BH}/dM + dI_{hH}/dM}{dI_{BH}/dM - dI_{hH}/dM}, \quad (8.3)$$

where the fitting functions have been used in place of the actual histograms in order to smooth out the oscillations. Notice that in the ratio the common factor s_α^2 cancels, therefore, the degree of cancellation between the two terms does not depend on the smallness of the heavy Higgs couplings.

In the region of the heavy resonance R is about 4%.

The two plots in the lower part provide the same information for the $2l2\nu jj$ final state with $M_H = 900$ GeV and $s_\alpha = 0.4$. Since now $s_\alpha^2 = 0.16$ is larger than in the previous example, the interference between the heavy scalar and the noHiggs amplitude is larger in absolute value than the interference between the two Higgs. As a consequence the sum is clearly non zero and agrees in sign with the former of the two interferences. In the region of the heavy resonance R is about 20%.

In order to appreciate these results, it is useful to compare them with the corresponding values for the $gg \rightarrow VV \rightarrow 4l, 2l2\nu$ case, which can be extracted from table 6 and table 8 of ref. [18]. Under the reasonable assumption that the light Higgs and background amplitudes vary little within one heavy Higgs width around the peak, the ratio of integrated interferences reproduce the ratio of amplitudes which define R , eq. (8.3). For the $gg \rightarrow ZZ \rightarrow 4l$, with $M_H = 600$ GeV and $s_\alpha = \sin(\pi/15) = 0.208$, one finds $R = 1.78$. For the $gg \rightarrow W^+W^- \rightarrow 2l2\nu$, with $M_H = 900$ GeV and $s_\alpha = \sin(\pi/8) = 0.383$, $R = 1.49$.

The vector bosons in the heavy Higgs decay, for all the masses we have considered, are predominantly longitudinally polarized. Unitarity requires that the leading term of the

contributions to jjV_LV_L production from vector boson interactions and the contribution from all Higgs exchanges must cancel each other exactly in the large energy limit, where vector and Higgs masses can be neglected. Subleading terms are not affected and therefore jjV_LV_L production is not necessarily zero. The near perfect suppression we observe between A_B and A_h , which results in a small interference of the heavy Higgs with the rest of the amplitude, suggests that the cancellation between A_B and A_h sets in already for invariant masses of the vector pair of a few hundred GeV, provided the mixing angle is not too large, an energy much smaller than the scale at which on shell V_LV_L scattering violates unitarity in a Higgsless theory.

From eq. (8.3) and eq. (8.1) one can extract the ratio of the two interferences, $R_{h/B}$

$$R_{h/B} = \frac{dI_{hH}/dM}{dI_{BH}/dM} = c_\alpha^2 \frac{dI_{hH}^{\text{SM}}/dM}{dI_{BH}/dM} = c_\alpha^2 R_{h/B}^0 = -\frac{1 - R/2}{1 + R/2}. \quad (8.4)$$

For $M_H = 600$ GeV and $s_\alpha = 0.2$, $R_{h/B} = -0.961$, while for $M_H = 900$ GeV and $s_\alpha = 0.4$, $R_{h/B} = -0.818$. Eq. (8.4) shows that, as the mixing angle α approaches zero, the ratio between the two interference terms approaches minus one. In fact, the values for $R_{h/B}^0$ in the two cases examined are -1.001 and -0.974 , respectively. In this limit, the heavy Higgs exchange amplitude is probing the cancellation between the Standard Model Higgs exchange and background amplitudes, which appears to be at the percent level.

9 Conclusions

We have studied Higgs sector interference effects in Vector Boson Scattering at the LHC, both in the Standard Model and its one Higgs Singlet extension as a prototype of theories in which more than one neutral, \mathcal{CP} even, scalars are present. We have concentrated on $pp \rightarrow jjl^+l^-l'^+l'^-$ and $pp \rightarrow jjl^-\bar{\nu}_l l'^+\nu_l$ production. We have shown that large interferences among the different Higgs exchange channels are present in the SM and that a production times decay approach fails to reproduce the off shell Higgs contribution. In the 1HSM, there are additional interferences between the two Higgs fields. Different approximations have been tried and proved inaccurate. We have found that the interference between the heavy Higgs diagrams and the rest of the amplitude, which is the sum of light Higgs exchange diagrams and of those diagrams in which no Higgs appear, is very small for values of the mixing angle compatible with the experimental constraints and can be neglected.

Acknowledgments

Several stimulating discussions with Anna Kropivnitskaya and Pietro Govoni are gratefully acknowledged. This work has been supported by MIUR (Italy) under contract 2010YJ2NYW_006, by the Compagnia di San Paolo under contract ORTO11TPXK and by the European Union Initial Training Network HiggsTools (PITN-GA-2012-316704).

Open Access. This article is distributed under the terms of the Creative Commons Attribution License ([CC-BY 4.0](https://creativecommons.org/licenses/by/4.0/)), which permits any use, distribution and reproduction in any medium, provided the original author(s) and source are credited.

References

- [1] ATLAS collaboration, *Observation of a new particle in the search for the Standard Model Higgs boson with the ATLAS detector at the LHC*, *Phys. Lett. B* **716** (2012) 1 [[arXiv:1207.7214](#)] [[INSPIRE](#)].
- [2] CMS collaboration, *Observation of a new boson at a mass of 125 GeV with the CMS experiment at the LHC*, *Phys. Lett. B* **716** (2012) 30 [[arXiv:1207.7235](#)] [[INSPIRE](#)].
- [3] CMS collaboration, *Precise determination of the mass of the Higgs boson and tests of compatibility of its couplings with the standard model predictions using proton collisions at 7 and 8 TeV*, *Eur. Phys. J. C* **75** (2015) 212 [[arXiv:1412.8662](#)] [[INSPIRE](#)].
- [4] ATLAS, CMS collaborations, *Combined Measurement of the Higgs Boson Mass in pp Collisions at $\sqrt{s} = 7$ and 8 TeV with the ATLAS and CMS Experiments*, *Phys. Rev. Lett.* **114** (2015) 191803 [[arXiv:1503.07589](#)] [[INSPIRE](#)].
- [5] ATLAS collaboration, *Updated coupling measurements of the Higgs boson with the ATLAS detector using up to 25 fb⁻¹ of proton-proton collision data*, *ATLAS-CONF-2014-009* (2014).
- [6] ATLAS collaboration, *Constraints on New Phenomena via Higgs Coupling Measurements with the ATLAS Detector*, *ATLAS-CONF-2014-010* (2014).
- [7] CMS collaboration, *Searches for new processes in the scalar sector at the CMS experiment*, *PoS(DIS2014)109* [[INSPIRE](#)].
- [8] N. Kauer and G. Passarino, *Inadequacy of zero-width approximation for a light Higgs boson signal*, *JHEP* **08** (2012) 116 [[arXiv:1206.4803](#)] [[INSPIRE](#)].
- [9] F. Caola and K. Melnikov, *Constraining the Higgs boson width with ZZ production at the LHC*, *Phys. Rev. D* **88** (2013) 054024 [[arXiv:1307.4935](#)] [[INSPIRE](#)].
- [10] J.M. Campbell, R.K. Ellis and C. Williams, *Bounding the Higgs width at the LHC using full analytic results for $gg \rightarrow e^-e^+\mu^-\mu^+$* , *JHEP* **04** (2014) 060 [[arXiv:1311.3589](#)] [[INSPIRE](#)].
- [11] J.M. Campbell, R.K. Ellis and C. Williams, *Bounding the Higgs width at the LHC: Complementary results from $H \rightarrow WW$* , *Phys. Rev. D* **89** (2014) 053011 [[arXiv:1312.1628](#)] [[INSPIRE](#)].
- [12] CMS collaboration, *Constraints on the Higgs boson width from off-shell production and decay to Z-boson pairs*, *Phys. Lett. B* **736** (2014) 64 [[arXiv:1405.3455](#)] [[INSPIRE](#)].
- [13] ATLAS collaboration, *Constraints on the off-shell Higgs boson signal strength in the high-mass ZZ and WW final states with the ATLAS detector*, *Eur. Phys. J. C* **75** (2015) 335 [[arXiv:1503.01060](#)] [[INSPIRE](#)].
- [14] CMS collaboration, *Limits on the Higgs boson lifetime and width from its decay to four charged leptons*, *Phys. Rev. D* **92** (2015) 072010 [[arXiv:1507.06656](#)] [[INSPIRE](#)].
- [15] J.M. Campbell and R.K. Ellis, *Higgs Constraints from Vector Boson Fusion and Scattering*, *JHEP* **04** (2015) 030 [[arXiv:1502.02990](#)] [[INSPIRE](#)].
- [16] C. Englert, Y. Soreq and M. Spannowsky, *Off-Shell Higgs Coupling Measurements in BSM scenarios*, *JHEP* **05** (2015) 145 [[arXiv:1410.5440](#)] [[INSPIRE](#)].
- [17] E. Maina, *Interference effects in Heavy Higgs production via gluon fusion in the Singlet Extension of the Standard Model*, *JHEP* **06** (2015) 004 [[arXiv:1501.02139](#)] [[INSPIRE](#)].

- [18] N. Kauer and C. O'Brien, *Heavy Higgs signal-background interference in $gg \rightarrow VV$ in the Standard Model plus real singlet*, *Eur. Phys. J. C* **75** (2015) 374 [[arXiv:1502.04113](#)] [[INSPIRE](#)].
- [19] C. Englert, I. Low and M. Spannowsky, *On-shell interference effects in Higgs boson final states*, *Phys. Rev. D* **91** (2015) 074029 [[arXiv:1502.04678](#)] [[INSPIRE](#)].
- [20] C. Englert and M. Spannowsky, *Limitations and Opportunities of Off-Shell Coupling Measurements*, *Phys. Rev. D* **90** (2014) 053003 [[arXiv:1405.0285](#)] [[INSPIRE](#)].
- [21] V. Silveira and A. Zee, *Scalar phantoms*, *Phys. Lett. B* **161** (1985) 136 [[INSPIRE](#)].
- [22] R. Schabinger and J.D. Wells, *A Minimal spontaneously broken hidden sector and its impact on Higgs boson physics at the large hadron collider*, *Phys. Rev. D* **72** (2005) 093007 [[hep-ph/0509209](#)] [[INSPIRE](#)].
- [23] D. O'Connell, M.J. Ramsey-Musolf and M.B. Wise, *Minimal Extension of the Standard Model Scalar Sector*, *Phys. Rev. D* **75** (2007) 037701 [[hep-ph/0611014](#)] [[INSPIRE](#)].
- [24] O. Bahat-Treidel, Y. Grossman and Y. Rozen, *Hiding the Higgs at the LHC*, *JHEP* **05** (2007) 022 [[hep-ph/0611162](#)] [[INSPIRE](#)].
- [25] V. Barger, P. Langacker, M. McCaskey, M.J. Ramsey-Musolf and G. Shaughnessy, *LHC Phenomenology of an Extended Standard Model with a Real Scalar Singlet*, *Phys. Rev. D* **77** (2008) 035005 [[arXiv:0706.4311](#)] [[INSPIRE](#)].
- [26] G. Bhattacharyya, G.C. Branco and S. Nandi, *Universal Doublet-Singlet Higgs Couplings and phenomenology at the CERN Large Hadron Collider*, *Phys. Rev. D* **77** (2008) 117701 [[arXiv:0712.2693](#)] [[INSPIRE](#)].
- [27] M. Gonderinger, Y. Li, H. Patel and M.J. Ramsey-Musolf, *Vacuum Stability, Perturbativity and Scalar Singlet Dark Matter*, *JHEP* **01** (2010) 053 [[arXiv:0910.3167](#)] [[INSPIRE](#)].
- [28] S. Dawson and W. Yan, *Hiding the Higgs Boson with Multiple Scalars*, *Phys. Rev. D* **79** (2009) 095002 [[arXiv:0904.2005](#)] [[INSPIRE](#)].
- [29] S. Bock, R. Lafaye, T. Plehn, M. Rauch, D. Zerwas and P.M. Zerwas, *Measuring Hidden Higgs and Strongly-Interacting Higgs Scenarios*, *Phys. Lett. B* **694** (2011) 44 [[arXiv:1007.2645](#)] [[INSPIRE](#)].
- [30] P.J. Fox, D. Tucker-Smith and N. Weiner, *Higgs friends and counterfeits at hadron colliders*, *JHEP* **06** (2011) 127 [[arXiv:1104.5450](#)] [[INSPIRE](#)].
- [31] C. Englert, T. Plehn, D. Zerwas and P.M. Zerwas, *Exploring the Higgs portal*, *Phys. Lett. B* **703** (2011) 298 [[arXiv:1106.3097](#)] [[INSPIRE](#)].
- [32] C. Englert, J. Jaeckel, E. Re and M. Spannowsky, *Evasive Higgs Maneuvers at the LHC*, *Phys. Rev. D* **85** (2012) 035008 [[arXiv:1111.1719](#)] [[INSPIRE](#)].
- [33] B. Batell, S. Gori and L.-T. Wang, *Exploring the Higgs Portal with 10/fb at the LHC*, *JHEP* **06** (2012) 172 [[arXiv:1112.5180](#)] [[INSPIRE](#)].
- [34] C. Englert, T. Plehn, M. Rauch, D. Zerwas and P.M. Zerwas, *LHC: Standard Higgs and Hidden Higgs*, *Phys. Lett. B* **707** (2012) 512 [[arXiv:1112.3007](#)] [[INSPIRE](#)].
- [35] R.S. Gupta and J.D. Wells, *Higgs boson search significance deformations due to mixed-in scalars*, *Phys. Lett. B* **710** (2012) 154 [[arXiv:1110.0824](#)] [[INSPIRE](#)].
- [36] B. Batell, D. McKeen and M. Pospelov, *Singlet Neighbors of the Higgs Boson*, *JHEP* **10** (2012) 104 [[arXiv:1207.6252](#)] [[INSPIRE](#)].

- [37] D. Bertolini and M. McCullough, *The Social Higgs*, *JHEP* **12** (2012) 118 [[arXiv:1207.4209](#)] [[INSPIRE](#)].
- [38] J.M. No and M. Ramsey-Musolf, *Probing the Higgs Portal at the LHC Through Resonant di-Higgs Production*, *Phys. Rev. D* **89** (2014) 095031 [[arXiv:1310.6035](#)] [[INSPIRE](#)].
- [39] G.M. Pruna and T. Robens, *Higgs singlet extension parameter space in the light of the LHC discovery*, *Phys. Rev. D* **88** (2013) 115012 [[arXiv:1303.1150](#)] [[INSPIRE](#)].
- [40] D. López-Val and T. Robens, *Δr and the W -boson mass in the singlet extension of the standard model*, *Phys. Rev. D* **90** (2014) 114018 [[arXiv:1406.1043](#)] [[INSPIRE](#)].
- [41] S. Profumo, M.J. Ramsey-Musolf, C.L. Wainwright and P. Winslow, *Singlet-catalyzed electroweak phase transitions and precision Higgs boson studies*, *Phys. Rev. D* **91** (2015) 035018 [[arXiv:1407.5342](#)] [[INSPIRE](#)].
- [42] C.-Y. Chen, S. Dawson and I.M. Lewis, *Exploring resonant di-Higgs boson production in the Higgs singlet model*, *Phys. Rev. D* **91** (2015) 035015 [[arXiv:1410.5488](#)] [[INSPIRE](#)].
- [43] T. Robens and T. Stefaniak, *Status of the Higgs Singlet Extension of the Standard Model after LHC Run 1*, *Eur. Phys. J. C* **75** (2015) 104 [[arXiv:1501.02234](#)] [[INSPIRE](#)].
- [44] H.E. Logan, *Hiding a Higgs width enhancement from off-shell $gg(\rightarrow h^*) \rightarrow ZZ$ measurements*, *Phys. Rev. D* **92** (2015) 075038 [[arXiv:1412.7577](#)] [[INSPIRE](#)].
- [45] V. Martín Lozano, J.M. Moreno and C.B. Park, *Resonant Higgs boson pair production in the $hh \rightarrow b\bar{b} WW \rightarrow b\bar{b}l^+\nu l^-\bar{\nu}$ decay channel*, *JHEP* **08** (2015) 004 [[arXiv:1501.03799](#)] [[INSPIRE](#)].
- [46] A. Falkowski, C. Gross and O. Lebedev, *A second Higgs from the Higgs portal*, *JHEP* **05** (2015) 057 [[arXiv:1502.01361](#)] [[INSPIRE](#)].
- [47] M. Ciccolini, A. Denner and S. Dittmaier, *Strong and electroweak corrections to the production of Higgs + 2jets via weak interactions at the LHC*, *Phys. Rev. Lett.* **99** (2007) 161803 [[arXiv:0707.0381](#)] [[INSPIRE](#)].
- [48] M. Ciccolini, A. Denner and S. Dittmaier, *Electroweak and QCD corrections to Higgs production via vector-boson fusion at the LHC*, *Phys. Rev. D* **77** (2008) 013002 [[arXiv:0710.4749](#)] [[INSPIRE](#)].
- [49] B. Jäger, C. Oleari and D. Zeppenfeld, *Next-to-leading order QCD corrections to $W+W$ -production via vector-boson fusion*, *JHEP* **07** (2006) 015 [[hep-ph/0603177](#)] [[INSPIRE](#)].
- [50] B. Jäger, C. Oleari and D. Zeppenfeld, *Next-to-leading order QCD corrections to Z boson pair production via vector-boson fusion*, *Phys. Rev. D* **73** (2006) 113006 [[hep-ph/0604200](#)] [[INSPIRE](#)].
- [51] B. Jäger, C. Oleari and D. Zeppenfeld, *Next-to-leading order QCD corrections to $W^+ W^+ jj$ and $W^- W^- jj$ production via weak-boson fusion*, *Phys. Rev. D* **80** (2009) 034022 [[arXiv:0907.0580](#)] [[INSPIRE](#)].
- [52] P. Bolzoni, F. Maltoni, S.-O. Moch and M. Zaro, *Higgs production via vector-boson fusion at NNLO in QCD*, *Phys. Rev. Lett.* **105** (2010) 011801 [[arXiv:1003.4451](#)] [[INSPIRE](#)].
- [53] P. Bolzoni, F. Maltoni, S.-O. Moch and M. Zaro, *Vector boson fusion at NNLO in QCD: SM Higgs and beyond*, *Phys. Rev. D* **85** (2012) 035002 [[arXiv:1109.3717](#)] [[INSPIRE](#)].
- [54] M. Cacciari, F.A. Dreyer, A. Karlberg, G.P. Salam and G. Zanderighi, *Fully Differential Vector-Boson-Fusion Higgs Production at Next-to-Next-to-Leading Order*, *Phys. Rev. Lett.* **115** (2015) 082002 [[arXiv:1506.02660](#)] [[INSPIRE](#)].

- [55] A. Ballestrero, A. Belhouari, G. Bevilacqua, V. Kashkan and E. Maina, *PHANTOM: A Monte Carlo event generator for six parton final states at high energy colliders*, *Comput. Phys. Commun.* **180** (2009) 401 [[arXiv:0801.3359](#)] [[INSPIRE](#)].
- [56] A. Ballestrero, D.B. Franzosi and E. Maina, *Vector-Vector scattering at the LHC with two charged leptons and two neutrinos in the final state*, *JHEP* **06** (2011) 013 [[arXiv:1011.1514](#)] [[INSPIRE](#)].
- [57] N.D. Christensen and C. Duhr, *FeynRules — Feynman rules made easy*, *Comput. Phys. Commun.* **180** (2009) 1614 [[arXiv:0806.4194](#)] [[INSPIRE](#)].
- [58] A. Alloul, N.D. Christensen, C. Degrande, C. Duhr and B. Fuks, *FeynRules 2.0 — A complete toolbox for tree-level phenomenology*, *Comput. Phys. Commun.* **185** (2014) 2250 [[arXiv:1310.1921](#)] [[INSPIRE](#)].
- [59] C. Degrande, C. Duhr, B. Fuks, D. Grellscheid, O. Mattelaer and T. Reiter, *UFO — The Universal FeynRules Output*, *Comput. Phys. Commun.* **183** (2012) 1201 [[arXiv:1108.2040](#)] [[INSPIRE](#)].
- [60] Ya. B. Zeldovich, I. Yu. Kobzarev and L.B. Okun, *Cosmological Consequences of the Spontaneous Breakdown of Discrete Symmetry*, *Zh. Eksp. Teor. Fiz.* **67** (1974) 3 [[INSPIRE](#)].
- [61] T.W.B. Kibble, *Topology of Cosmic Domains and Strings*, *J. Phys. A* **9** (1976) 1387 [[INSPIRE](#)].
- [62] T.W.B. Kibble, *Some Implications of a Cosmological Phase Transition*, *Phys. Rept.* **67** (1980) 183 [[INSPIRE](#)].
- [63] S.A. Abel, S. Sarkar and P.L. White, *On the cosmological domain wall problem for the minimally extended supersymmetric standard model*, *Nucl. Phys. B* **454** (1995) 663 [[hep-ph/9506359](#)] [[INSPIRE](#)].
- [64] A. Friedland, H. Murayama and M. Perelstein, *Domain walls as dark energy*, *Phys. Rev. D* **67** (2003) 043519 [[astro-ph/0205520](#)] [[INSPIRE](#)].
- [65] V. Barger, P. Langacker, M. McCaskey, M. Ramsey-Musolf and G. Shaughnessy, *Complex Singlet Extension of the Standard Model*, *Phys. Rev. D* **79** (2009) 015018 [[arXiv:0811.0393](#)] [[INSPIRE](#)].
- [66] LHC Higgs Cross Section Working Group collaboration, J.R. Andersen et al., *Handbook of LHC Higgs Cross Sections: 3. Higgs Properties*, [arXiv:1307.1347](#) [[INSPIRE](#)].
- [67] J. Pumplin, D.R. Stump, J. Huston, H.L. Lai, P.M. Nadolsky and W.K. Tung, *New generation of parton distributions with uncertainties from global QCD analysis*, *JHEP* **07** (2002) 012 [[hep-ph/0201195](#)] [[INSPIRE](#)].
- [68] M. Szleper, *The Higgs boson and the physics of WW scattering before and after Higgs discovery*, [arXiv:1412.8367](#) [[INSPIRE](#)].